

Submitted to The Astronomical Journal

WISE photometry for 400 million SDSS sourcesDustin Lang^{1,2,3}, David W. Hogg^{4,5}, David J. Schlegel⁶**ABSTRACT**

We present photometry of images from the Wide-Field Infrared Survey Explorer (WISE; Wright *et al.* 2010) of over 400 million sources detected by the Sloan Digital Sky Survey (SDSS; York *et al.* 2000). We use a “forced photometry” technique, using measured SDSS source positions, star–galaxy separation and galaxy profiles to define the sources whose fluxes are to be measured in the WISE images. We perform photometry with *The Tractor* image modeling code, working on our “unWISE” coaddeds and taking account of the WISE point-spread function and a noise model. The result is a measurement of the flux of each SDSS source in each WISE band. Many sources have little flux in the WISE bands, so often the measurements we report are consistent with zero. However, for many sources we get three- or four-sigma measurements; these sources would not be reported by the WISE pipeline and will not appear in the WISE catalog, yet they can be highly informative for some scientific questions. In addition, these small-signal measurements can be used in *stacking* analyses at catalog level. The forced photometry approach has the advantage that we measure a *consistent* set of sources between SDSS and WISE, taking advantage of the resolution and depth of the SDSS images to interpret the WISE images; objects that are resolved in SDSS but blended together in WISE still have accurate measurements in our photometry. Our results, and the code used to produce them, are publicly available at <http://unwise.me>.

¹McWilliams Center for Cosmology, Department of Physics, Carnegie Mellon University, 5000 Forbes Ave, Pittsburgh, PA, 15213, USA

²Department of Physics & Astronomy, University of Waterloo, 200 University Avenue West, Waterloo, ON, N2L 3G1, Canada

³To whom correspondence should be addressed: dstn@cmu.edu

⁴Center for Cosmology and Particle Physics, Department of Physics, New York University, 4 Washington Place, New York, NY, 10003, USA

⁵Max-Planck-Institut für Astronomie, Königstuhl 17, D-69117, Heidelberg, Germany

⁶Lawrence Berkeley National Laboratory, 1 Cyclotron Road, Berkeley, CA, 94720, USA

Subject headings: methods: data analysis — surveys — techniques: image processing

1. Introduction

In astronomical survey projects, it is common practice to produce a *catalog* of detected and measured sources, using only data from the survey itself. This approach has the benefit that the survey can be thought of as an independent experiment, but the disadvantage that it ignores the huge amount of information we already have about astronomical sources measured in previous surveys covering the same part of the sky. While new surveys typically bring some new capability that previous surveys lacked (eg, depth, resolution, or wavelength coverage), it is seldom the case that a new survey surpasses all previous data in all regards; there is usually some complementary information that could be of value.

This approach of compiling “independent” catalogs has two shortcomings, in particular when it comes to comparing the new survey with existing surveys. First, when the new survey has lower resolution, there will be some nearby sets of sources that are blended together (detected and measured as a single source) in the new catalog, but resolved in existing data. Second, when the new survey has lower sensitivity (at least to some types of sources), sources known from previous surveys will not be detected in the new survey and will not appear in its catalog. When investigators attempt to cross-match the new catalog with existing catalogs (usually via astrometric cross-matching), the first problem (blended sources) typically results in either failed matches (because the blended source has a different centroid), or very strange inferred properties (for example, bizarre colors because the new survey matches the sum of a set of sources to a single source in the existing survey; or unexpected non-matching sources). The second problem (non-detections) means that fewer sources are available to cross-match; a catalog cross-match is limited by the weaknesses of both catalogs.

In contrast, in this paper we perform “forced photometry” of a new survey (WISE) given a great deal of knowledge from an existing survey (SDSS). While WISE has comparable *depth* to SDSS for many sources, its resolution is significantly lower. We therefore get significant benefit from using SDSS detections to decide *where to look* in the WISE data.

The Wide-Field Infrared Survey Explorer (WISE; Wright *et al.* 2010) measured the full sky in four mid-infrared bands centered on 3.4 μm , 4.6 μm , 12 μm , and 22 μm , known as W1 through W4. During its primary mission, it scanned the full sky in all four bands. After its solid hydrogen cryogen ran out and W4 became unusable, it continued another half-sky

scan in W1, W2, and W3. During the “NEOWISE post-cryo” continuation (Mainzer *et al.* 2011), it continued to scan another half-sky in W1 and W2. Over 99% of the sky has 11 or more exposures in W3 and W4, and 23 or more exposures in W1 and W2. Median coverage is 33 exposures in W1 and W2, 24 in W3, and 16 in W4. In December 2013, WISE was reactivated and is expected to complete several more full scans of the sky in W1 and W2 (Mainzer *et al.* 2014).

The WISE team have made a series of high-quality data releases, the most recent of which is the AllWISE Data Release.¹ The AllWISE Release includes a source catalog of nearly 750 million sources, a database of photometry in the individual frames at each source position, and “Atlas Images”: coadded matched-filtered images. The AllWISE Atlas Images were intentionally convolved by the point-spread function (PSF), making it challenging to use them for forced photometry. Instead, we use the “unWISE” coadds from Lang (2014), which preserve the resolution of the original WISE images.

The Sloan Digital Sky Survey (SDSS; York *et al.* 2000) imaged over 14,000 square degrees of sky in five bands (u, g, r, i, z), detecting and measuring over 400 million sources. We use the imaging catalogs from SDSS-III Data Release 10 (Eisenstein *et al.* 2011; Ahn *et al.* 2013). These catalogs contain the outputs of the *Photo* pipeline (Lupton *et al.* 2001), and include star/galaxy separation and galaxy shape measurements using either exponential, de Vaucouleurs, or composite (sum of exponential and de Vaucouleurs) profiles.

The combination of data from SDSS and WISE has proven to be very powerful for a variety of studies. Yan *et al.* (2013) give a survey of the properties of extragalactic sources, showing that SDSS–WISE colors and morphology can be used to select type-2 dust-obscured quasars and ultra-luminous infrared galaxies at redshift ~ 2 . The SDSS-III BOSS survey (Dawson *et al.* 2013) includes quasars targeted using SDSS color cuts and WISE detection in the W1, W2, and W3 bands, to select $z > 2$ quasars.

The work described here was motivated by the need to select targets for the SDSS-III SEQUELS and SDSS-IV eBOSS programs. Myers *et al.* (in prep.) describe the use of our results to select quasars, while Prakash *et al.* (in prep.) describe the selection of luminous red galaxy (LRG) targets. The LRG targets are fairly bright in WISE, so a catalog match produces satisfactory results. However, due to the lower resolution of the WISE images, nearby sources that are resolved in SDSS may be blended in WISE, resulting either in missed astrometric matches (because the WISE centroid is shifted), or incorrect colors (because the WISE catalog source includes flux from multiple SDSS sources). Using our results improves

¹Explanatory Supplement to the AllWISE Data Release Products, <http://wise2.ipac.caltech.edu/docs/release/allwise/expsup/>

this situation, since we photometer a consistent set of sources. For the quasar targets, the often few-sigma flux measurements we make are of considerable utility. In the redshift range of interest, the quasar and stellar loci are significantly separated in SDSS–WISE colors, so even a noisy measurement of the WISE flux can effectively eliminate stellar contamination.

In similar work, the “extreme deconvolution” quasar target selection and redshift-estimation method (XDQSOz; Bovy *et al.* 2012) makes effective use of forced photometry of GALEX UV (Martin *et al.* 2005) and UKIDSS near-IR (Lawrence *et al.* 2007) images, based on SDSS source positions. While often low-signal-to-noise, these measurements nevertheless can be very effective in eliminating degeneracies in quasar classification and redshift determination. Indeed, the XDQSOz method has been extended to incorporate the measurements we present here by DiPompeo *et al.* (in prep).

2. Method

We use *the Tractor* code (Lang *et al.*, in prep.) in “forced photometry” mode. In general, *the Tractor* optimizes or samples from a full generative model that includes parameters of the image calibration and all the parameters of the sources in the images (positions, shapes, and fluxes). In forced photometry mode, the image calibration parameters are frozen (held fixed), as are all properties of the sources except for their fluxes in the bands of interest. In this case, the photometry task becomes linear: We know what each source should look like in the WISE images, and we must compute the linear sum of the sources that best matches the observed image.

The image calibration parameters include the astrometric calibration, described by a World Coordinate System (WCS); the photometric calibration, described by a zeropoint; a point-spread function model; a noise model (per-pixel error estimates); and a “sky” or background model. We are photometering the “unWISE” coadds, which are tiles of roughly $1.5^\circ \times 1.5^\circ$ in extent. The tiles use a gnomonic projection (tangent plane; WCS code “TAN”), are sky-subtracted, and have a photometric zeropoint of 22.5 in the Vega system. In turn, these coadds use the “level 1b” calibrated individual exposures from the WISE All-Sky Data Release. We use the WISE PSF models from the WISE All-Sky Release,² averaged over the focal plane and approximated by a mixture of three isotropic concentric Gaussian components. We have been impressed by the quality of the WISE PSF models from Meisner *et al.*

²Available at http://wise2.ipac.caltech.edu/docs/release/allsky/expsup/sec4_4c.html#psf

(2014),³ but have opted to use the WISE team’s models here for consistency. Figure 1 shows the AllWISE PSF models and our Gaussian approximations. Table 1 lists the parameters of our PSF models.

For an example of the forced photometry results, see Figure 2.

We photometer sources in the SDSS DR10 imaging catalog.⁴ We select “survey primary” sources (those detected in the “best” imaging scan covering each part of the sky) from the *photoObj* catalog files. We drop the “parent” sources in blends, keeping the deblended children. We use the *r*-band galaxy shape measurements. We find that many faint sources classified as galaxies have poorly constrained galaxy shape measurements. We treat these as point sources rather than galaxies in our photometry. Specifically, we treat as a point source any galaxy whose effective radius is measured at a signal-to-noise of less than 3; or with stated axis ratio error of zero; or with the maximum effective radius considered by the *Photo* software; or with stated effective radius signal-to-noise significantly greater than expected given its flux; or with magnitude $r < 12.5$ (bright stars whose PSF wings are mistakenly identified as galaxies). Examples of sources we treat as point sources are shown in Figure 3.

For each WISE tile, we keep SDSS sources that are within the tile plus a margin of 20 WISE pixels (55 arcseconds). We also include in the fitting sources that are detected in the AllWISE Release catalog but not SDSS; we keep WISE catalog sources that have no SDSS match within 4 arcseconds.

The *Tractor* code proceeds by rendering the galaxy or point source models convolved by the image PSF model. The galaxy profiles are represented as mixtures of Gaussians, as described in Hogg & Lang (2012), and we fit a mixture of Gaussians to the PSF model. The convolution is then analytic and rendering PSF-convolved galaxy profiles becomes a matter of evaluating a large number of Gaussians. In principle these Gaussian profiles have infinite extent, but we clip them when the surface brightness drops below approximately 10% of the per-pixel noise. Once the profile of each source has been rendered, forced photometry requires performing a linear least-squares fit for source fluxes such that their sum is closest to the actual image pixels, with respect to the noise model. This least-squares problem is very sparse (most sources touch only dozens of pixels); the *Tractor* uses *Ceres Solver* (Agarwal *et al.* 2012), which handles this case well, as its optimization engine for forced photometry.

³Available at <https://github.com/ameisner/WISE/>

⁴We have also photometered what will become the DR13 catalog, and will release these results when DR13 is released. For our purposes, these data releases differ only in their choice of which field to call “primary”; the precise set of objects photometered will differ in some parts of the sky.

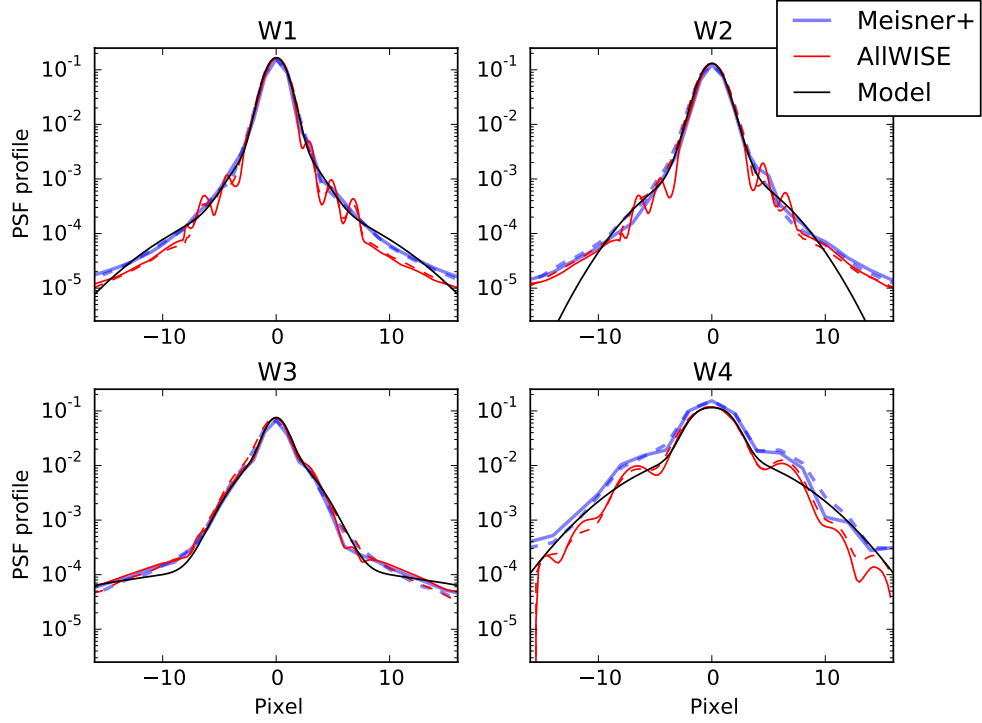


Fig. 1.— PSF models from the AllWISE Release, from Meisner *et al.* 2014, and our three-component, zero-mean, isotropic, concentric Gaussian fits. Note the log scale. The AllWISE and Meisner *et al.* 2014 plots are horizontal (solid) and vertical (dashed) slices through the PSF center. Our mixture-of-Gaussian models capture the PSF cores—roughly three orders of magnitude—quite effectively, but degrade somewhat at large radii and low flux levels.

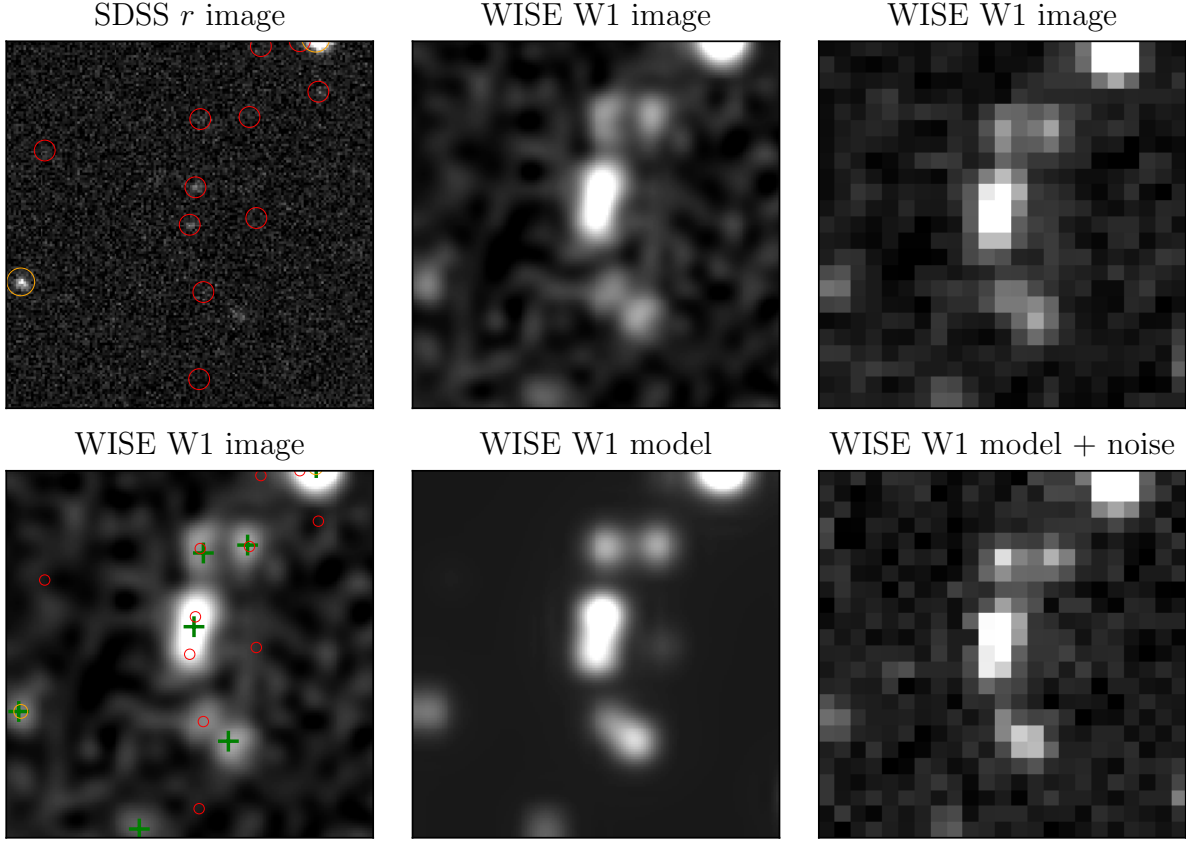


Fig. 2.— Example forced photometry results. **Top-left:** SDSS r -band image, with point sources (small red) and galaxies (large orange) marked. (Some of these sources will have been detected in the other SDSS bands.) These are the sources that will be photometered, along with sources from the WISE catalog that are detected only in WISE. **Top-middle:** WISE W1 image, smoothed by resampling. **Top-right:** WISE W1 image at original (native) resolution. **Bottom-left:** WISE W1 image, with WISE catalog detections (green cross) and SDSS sources marked. Notice that the central source is detected as a single source in WISE, but resolved into two sources by SDSS. Also notice a number of WISE-only and SDSS-only detections. **Bottom-middle:** Forced photometry model image. This is a weighted sum of WISE PSF models (convolved by the galaxy profile for the one galaxy in this field) at the positions of SDSS and WISE-only sources, with weights chosen to minimize the chi-squared residuals from the WISE W1 image. **Bottom-right:** The model image at native resolution, plus per-pixel noise equal to that in the real image. The model is a good approximation to the real image, given the observational noise.

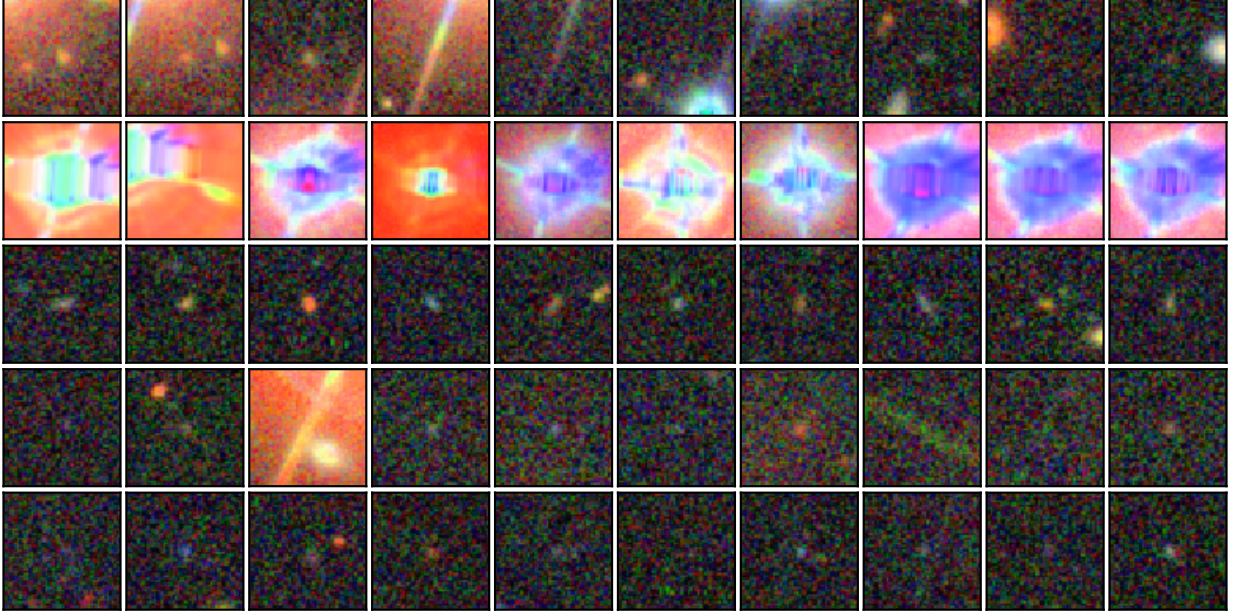


Fig. 3.— Examples of SDSS sources that we treat as point sources for photometry. Each image is a 50×50 cutout in SDSS *irg* bands.

Top row: effective radius measured at a signal-to-noise less than 3.

Second row: sources with large flux (stars).

Third row: axis ratio has a reported error of zero.

Fourth row: effective radius reported is the largest allowed.

Bottom row: effective radius signal-to-noise is larger than expected given the measured flux of the object.

We photometer each WISE tile and each WISE band separately. Since the WISE tiles overlap slightly, this means we photometer some SDSS sources in multiple tiles. We resolve these multiple measurements after processing all tiles, keeping only the measurement closest to the center of its tile. We then write out files that are row-by-row parallel to the SDSS *photoObj* input files. The contents of our catalogs are described in Appendix A.

3. Results

We photometered a total of 7,989 WISE tiles, covering roughly 14,900 square degrees and containing roughly 469 million SDSS sources. The AllWISE catalog contains roughly 240 million sources in the same area. Of the 469 million sources photometered, we treated

430 million as point sources and 34 million as galaxies. Photometry took roughly 1500 CPU-hours total.

3.1. Comparison to WISE catalog

Comparisons between our results and the “official” WISE catalog are shown in Figures 4, 5, 6, 7, and 8. For isolated point sources, our results are consistent to within about 0.03 mag. A slight tilt is evident, similar to the tilt seen in the comparison of the All-Sky and AllWISE releases. We expect this is due to photometric calibration differences between the All-Sky and AllWISE releases. Unfortunately, the AllWISE “level 1b” calibrated exposures have not been released, so improving this effect is beyond the scope of this work.

3.2. Sources undetected in the WISE catalog

Figure 9 shows a comparison between our forced-photometry results as compared to a traditional approach of astrometric matching between the SDSS and WISE catalogs. The traditional approach demands that all sources be detected in both catalogs, while our approach allows few-sigma WISE sources to be measured. For some science cases, these few-sigma measurements can be very useful, either individually or in stacking analyses. In addition, we photometer more source overall, since often SDSS resolves nearby sources that are blended in WISE.

3.3. Artifacts

Figure 10 shows a comparison of the artifacts around bright stars in our forced-photometry results and the AllWISE catalog. The most notable effect is a significant halo: sources in the SDSS catalog that we report as being bright. This occurs because our PSF models (as shown in Figure 1) focus on the core, largely ignoring the wings of the PSF. In our forced photometry approach, when this unexplained flux coincides with a source, the least-squares fitter will try to “explain” the extra flux by making the source brighter. As a result, any source near a bright star will appear too bright in our results. The examples shown in Figure 10 are among the brightest stars in our footprint, and for these stars the halo can be 10 arcminutes or larger.

Table 1. Mixture-of-Gaussian PSF fit parameters. The rows list the three Gaussian components we use to represent the PSF. “Amp” indicates the amplitude or “weight” of the component, and “Std” is the standard deviation of the Gaussian. Notice that for W4, one of the components is negative; while perhaps surprising, the resulting PSF is still positive everywhere so this is not an issue. Also notice that the sums of amplitudes are not strictly unity.

Component	W1		W2		W3		W4	
	Amp	Std	Amp	Std	Amp	Std	Amp	Std
1	0.7610	0.8664	0.5007	0.8972	0.2752	0.8555	−0.2929	1.1001
2	0.1538	2.1499	0.3410	1.3302	0.5537	2.3620	0.7035	1.3284
3	0.0723	5.8201	0.1344	3.7869	0.1461	13.3751	0.6207	5.0750

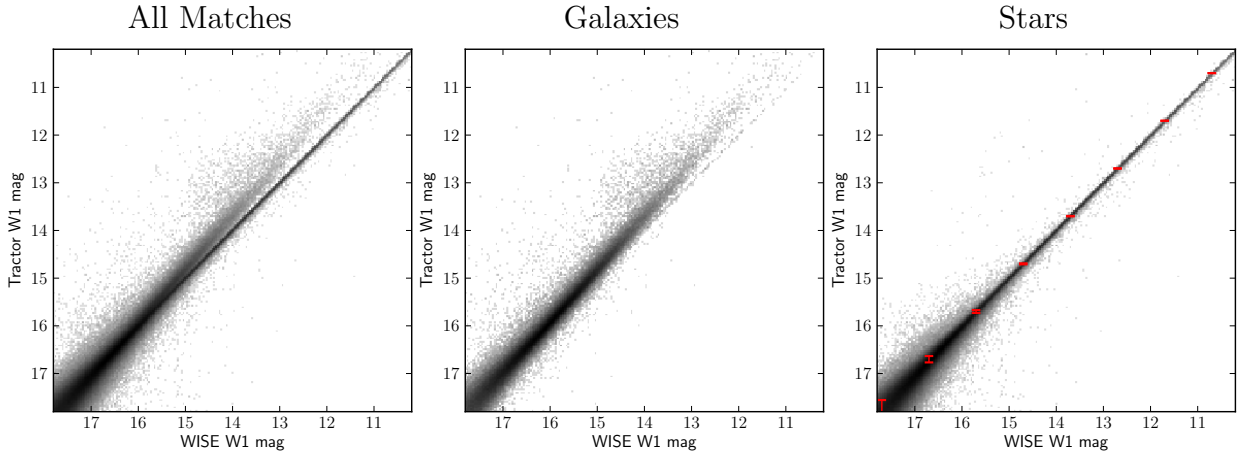


Fig. 4.— Comparison of our forced photometry magnitudes and WISE AllWISE Release catalog magnitudes, in W1, for matched sources within 4 arcseconds, in ~ 100 square degrees of sky around RA,Dec = (180, 45). We show only unique (one-to-one) matches, since otherwise the *Tractor* photometry resolves sources that are blended in WISE. **Left:** All sources; **Middle:** Sources identified in the SDSS imaging as galaxies, and not treated as point sources in our photometry; **Right:** sources identified by SDSS as point-like, plus nominally extended sources treated as point sources in our photometry. The error bars shown are the median WISE catalog error bars per magnitude bin. The WISE catalog magnitude entry we are plotting is *w1mpro*, a point-source measurement; this explains why the *Tractor* measurements of galaxies tend to be brighter: we measure all the galaxy’s flux, while the WISE catalog only measures the fraction in the point-like core.

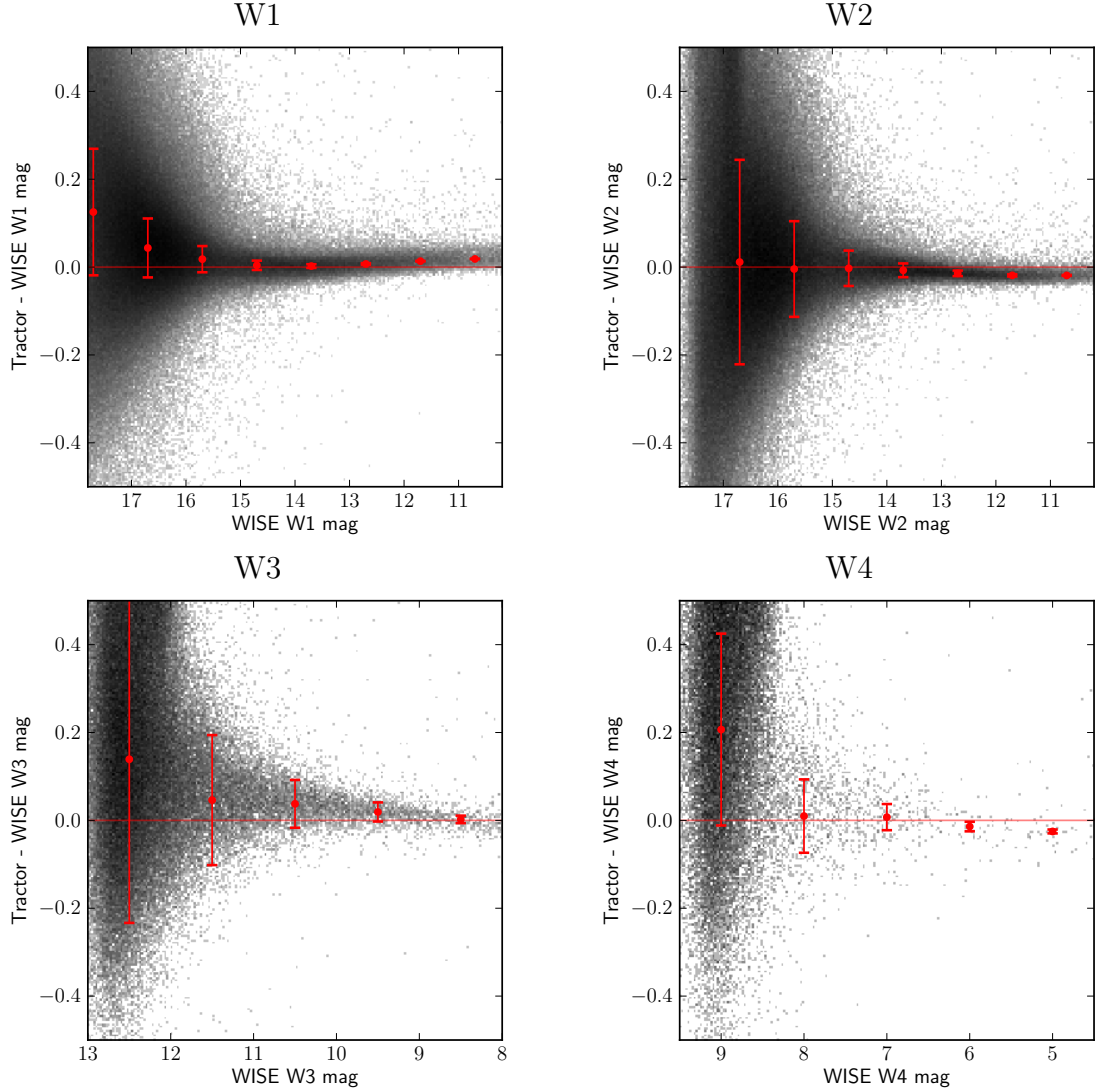


Fig. 5.— Comparison of our forced photometry magnitudes and WISE AllWISE Release catalog magnitudes, for sources treated as point sources in our photometry. These are sources in the same ~ 100 square degrees in Figure 4. The slight tilts seen are comparable in magnitude to the differences between the All-Sky and AllWISE releases, and may be due to differences in photometric calibration between the releases.

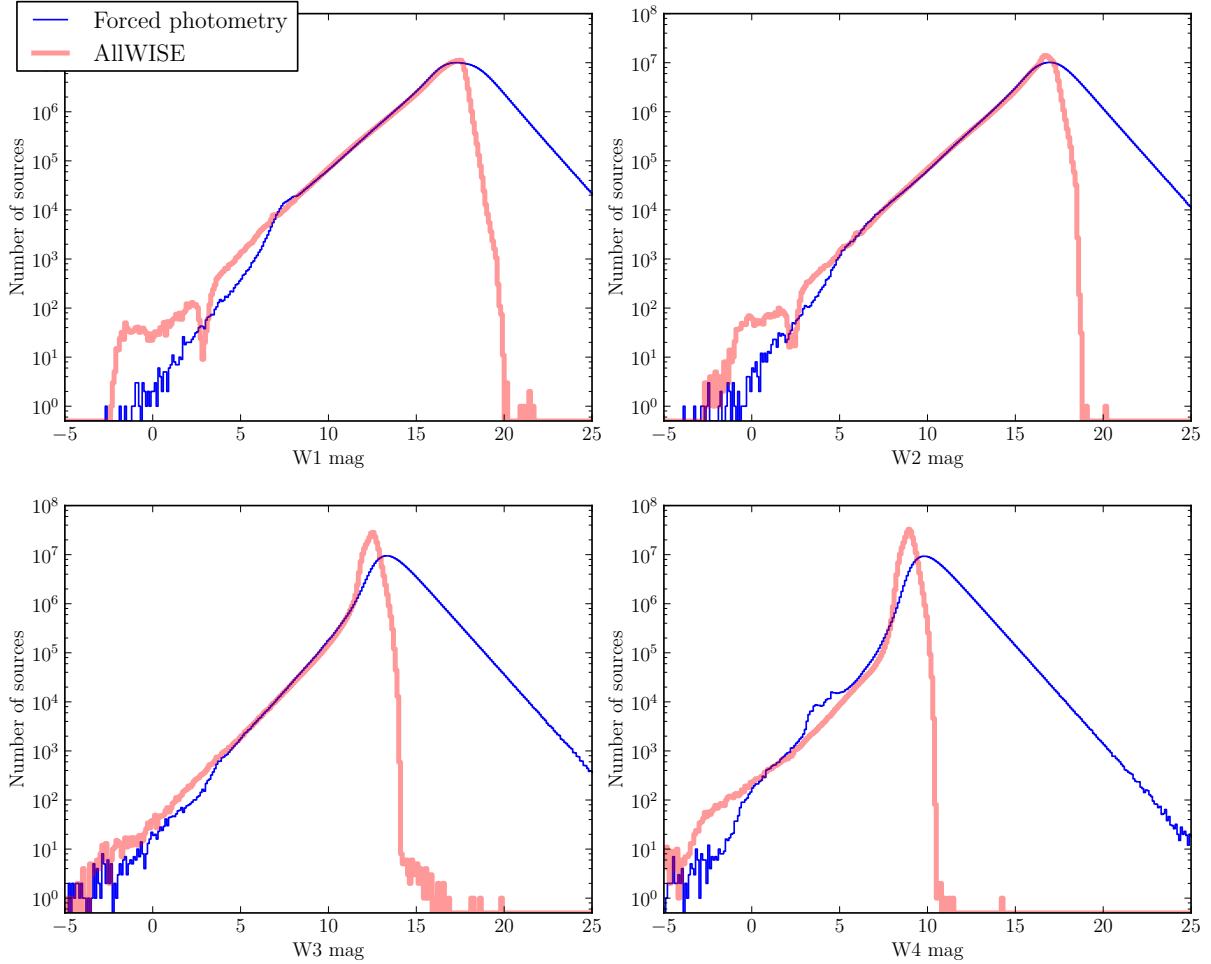


Fig. 6.— Comparison of our forced photometry magnitudes and WISE AllWISE Release catalog magnitudes. **Top-left:** W1. Observe that above W1 mag ~ 17 , the AllWISE catalog detection efficiency drops sharply. Our forced photometry results, in contrast, include faint measurements of many more sources (albeit at low signal-to-noise). An unusual deficit of AllWISE sources around mag ~ 3 is apparent, while our forced photometry results show a rather smooth distribution. The shape of the forced photometry distribution should be essentially the convolution of the SDSS optical detection efficiency and the optical–WISE colors. **Top-right:** W2 is similar. **Bottom-left:** W3. The AllWISE catalogs shows an upturn in number of sources of mag 11 to 12. **Bottom-right:** W4 shows a similar effect.

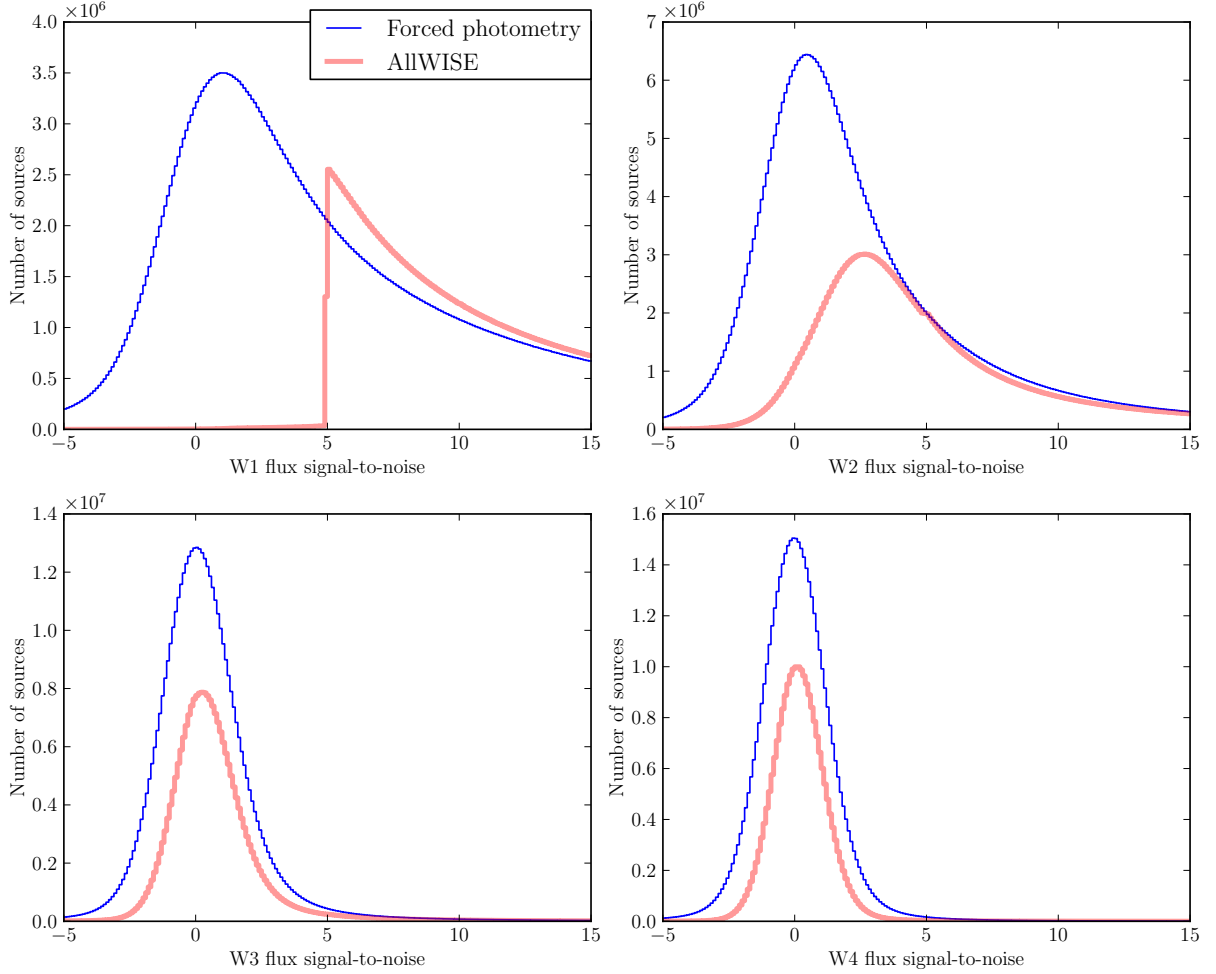


Fig. 7.— Comparison of our forced photometry magnitudes and WISE AllWISE Release signal-to-noise distributions. **Top-left:** W1. Since WISE is most sensitive in W1, the AllWISE catalog is essentially W1-selected. As a result, the W1 measurements rise sharply at the W1 detection threshold. Our forced photometry results, in contrast, include measurements of sources below the detection threshold. **Top-right:** W2. Our results for bright sources follow those of the AllWISE catalog, but we include more faint measurements. **Bottom-left:** W3 and **Bottom-right:** W4 are similar.

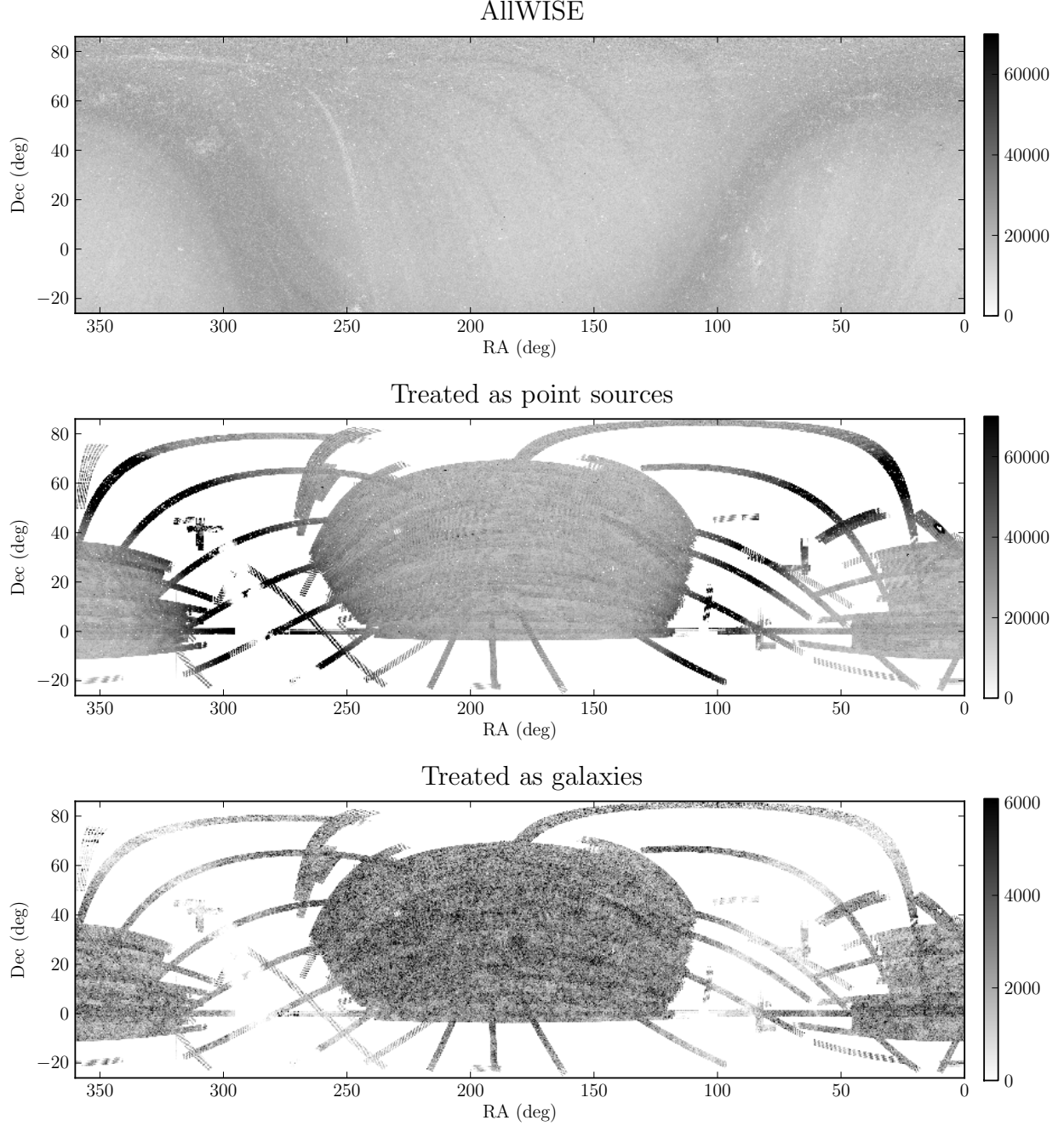


Fig. 8.— Spatial distribution of measurements. **Top:** objects in the AllWISE catalog. **Center:** objects in our forced photometry results that were treated as point sources. **Bottom:** sources we treated as galaxies. The units are sources per square degree; note that we only treat $\sim 10\%$ of the sources as galaxies.

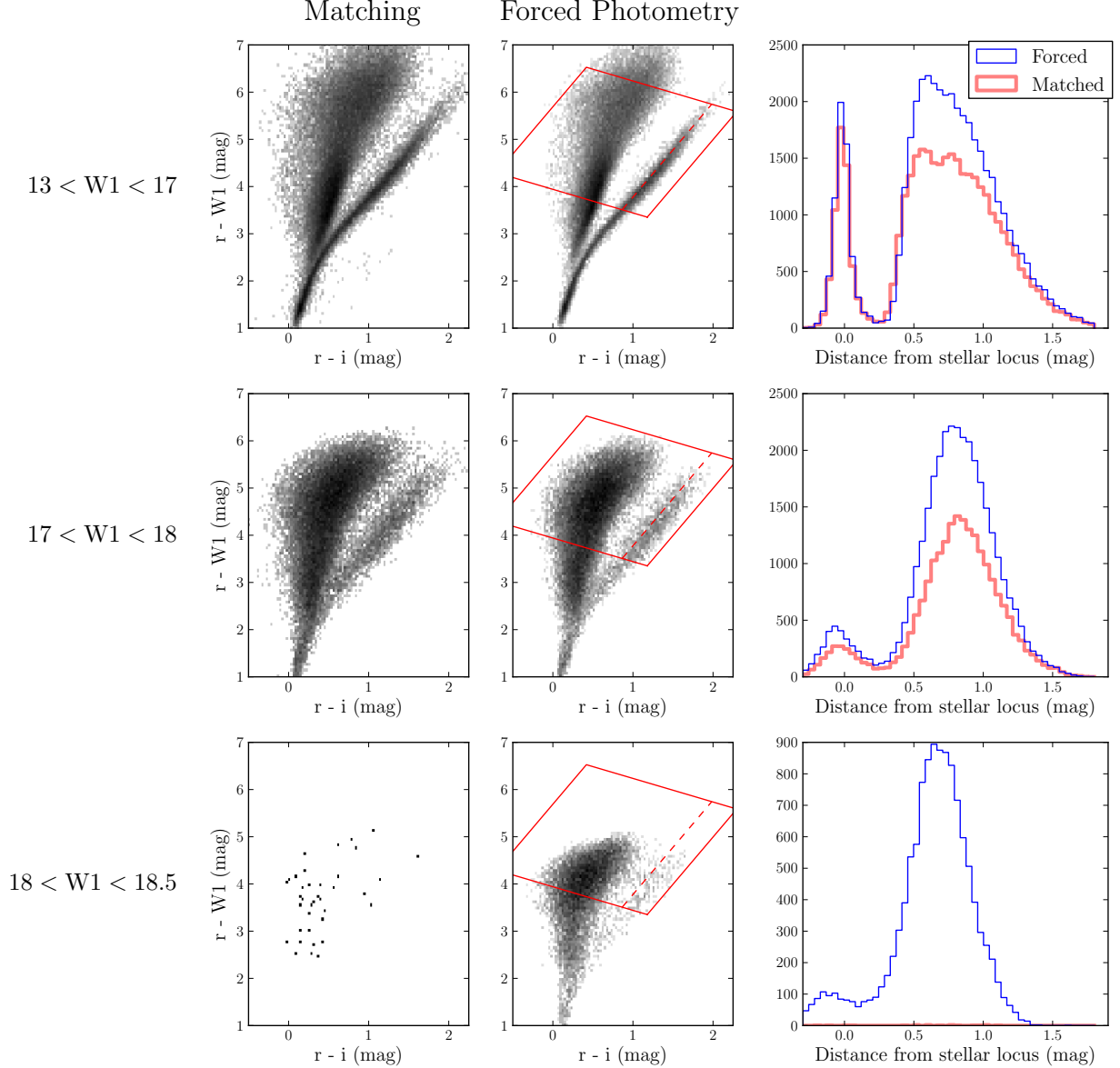


Fig. 9.— Comparison between our forced-photometry measurements and traditional astrometric matching to the WISE catalog. The $r - W1$ vs $r - i$ color-color plane is used for the selection of luminous red galaxy (LRG) targets in the SDSS-III/SEQUELS survey. **Top:** bright sources. **Middle:** moderate sources. **Bottom:** faint sources in W1. The scatterplots show the density of sources in color-color space, using astrometric matching (left) or our forced photometry results (middle). The histogram (right) shows the distance of sources from the approximate stellar locus location (dashed line), within the indicated box. For the bright sources, the results are similar, but we measure overall more sources thanks to the resolving power of SDSS. At moderate brightness, we again get similar results. The bump of sources near the stellar locus is broader due to photometric errors. At faint brightness levels, the sources are not detected in WISE alone, so do not appear in the WISE catalog and cannot be matched. In contrast, our photometric measurements remain reasonable below the WISE detection threshold and allow reliable separation of stars and LRG targets.

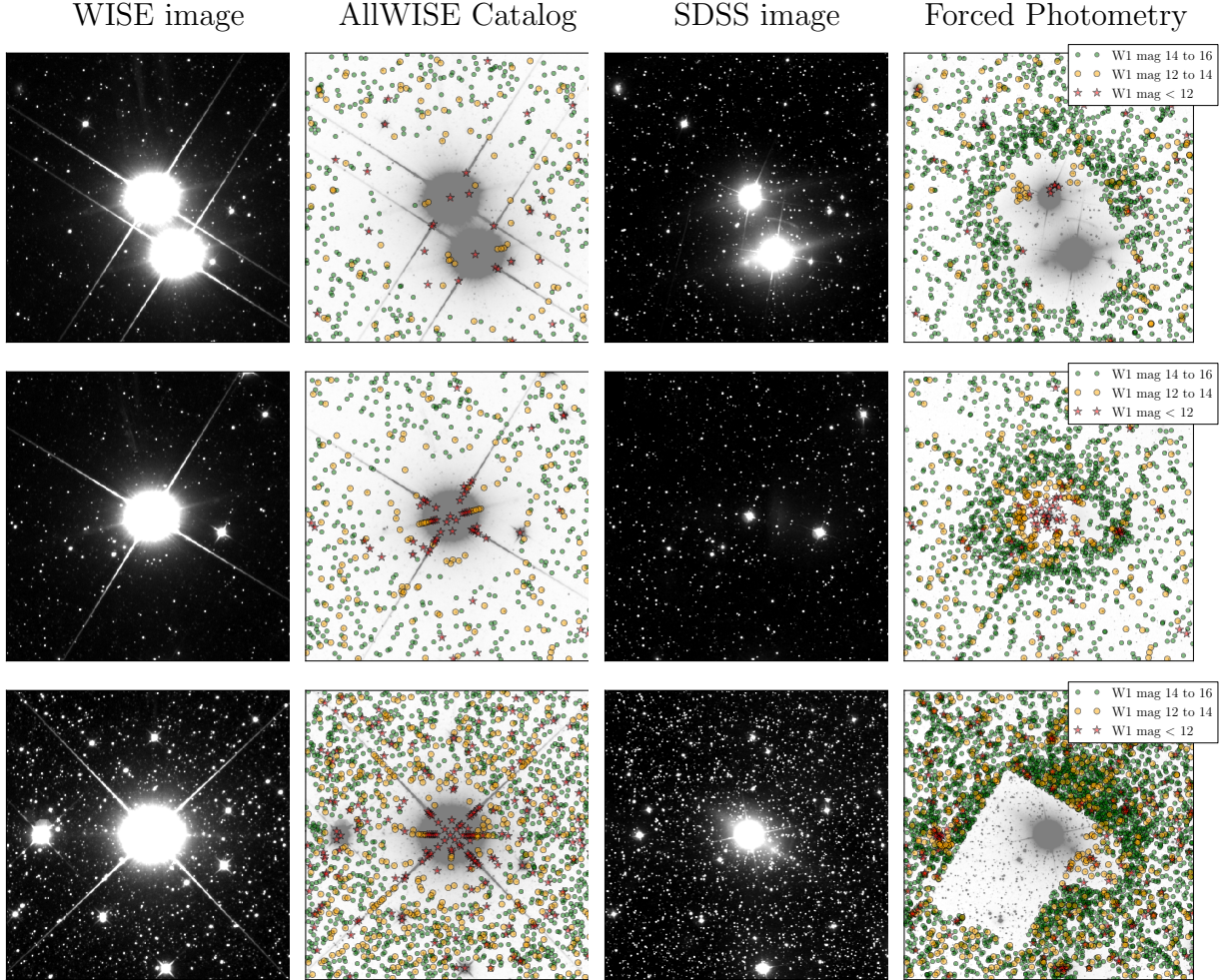


Fig. 10.— Effects of bright stars on our forced photometry results. **Left column:** WISE W1 images around bright stars. These images are 24×24 arcminutes in size. **Second column:** AllWISE catalog entries nearby. Notice the lack of moderate-brightness sources near the bright source, and the small number of bright artifact sources. **Third column:** SDSS r -band image. **Right column:** our forced-photometry results. In the top row, there is a region near the bright star that contains few sources in the SDSS catalog (and hence in our forced photometry results), a handful of sources measured as being very bright, and a “halo” of moderately bright sources outside the empty region. In the middle row, the halo of bright measurements is very pronounced; the WISE diffraction spikes are also apparent. In the bottom row, the bright star causes the SDSS image reduction pipeline to fail, so there are no sources in that field. These examples show extremely bright stars ($W1 \sim -2$); fainter stars show more moderate artifacts.

4. Discussion

Forced photometry is one approach for applying information learned in one survey to data gathered in a second survey. It is rigid, in the sense that we *only* photometer the images at locations containing a source in the input catalog. As such, forced photometry is most useful when the survey providing the catalog of sources to photometer has at least the depth and resolution of the images being photometered. In addition, forced photometry demands that the images being photometered are well calibrated. While it is possible to fit for the PSF model, astrometric solution and sky level using *the Tractor*, this incurs additional computational cost and is not necessarily the most efficient approach for recalibrating images. We are fortunate that the WISE team have produced superbly calibrated images so that image recalibration has been unnecessary.

A more holistic approach than forced photometry would be to do *simultaneous fitting*. We could, for instance, fit all parameters of the sources (galaxy shapes and positions as well as fluxes), and include both the SDSS and WISE images in the fitting. This would extract additional information from both surveys, yielding stronger constraints on the source properties. It would also allow fitting for proper motions and parallaxes of nearby stars. In addition, we could detect sources that are below the individual survey detection thresholds but are significant when the surveys are combined. This approach would, however, be significantly more computationally expensive: To start, SDSS images have roughly 50 times more pixels per area than WISE. Further, this would require non-linear optimization, in contrast to the much cheaper linear optimization required by forced photometry. Since we do not expect the WISE images (with their lower resolution) to have much constraining power on the positions or shapes of galaxies, an alternative approach would be first to re-fit the SDSS catalog to the SDSS images using *the Tractor*, and then repeat our forced photometry with that improved catalog. For moving sources, we could search for regions of the WISE images that are poorly fit by the SDSS catalog and allow the sources in these regions to shift their positions slightly. This post-processing approach would allow us to improve upon the forced photometry results without increasing the computational cost excessively.

In this work, we have used coadds of the WISE imaging, rather than the individual frames. While in general it would be preferable to photometer the individual frames (at least in principle), the WISE images have a stable and approximately isotropic PSF with little variation over the focal plane, so little information is lost in the coadding process. The computational time and memory requirements scale roughly with the number of pixels being fit, so photometering the individual frames would have cost roughly 30 times more.

Forced photometry assumes that the profile of a galaxy is the same between bands. This does not describe the (typically small) color gradients across galaxies, although the

WISE images lack the resolution to inform any such gradients in the infrared colors. Our forced photometry of the WISE fluxes is equivalent to a weighted-aperture flux that has the property of being well-defined and consistently applied to all objects. Therefore, any biases in the inferred infrared fluxes would be consistent between galaxies that have the same intrinsic properties.

In this paper, we used the SDSS r -band galaxy shape measurements as the galaxy profiles for forced photometry. One might expect the z -band shapes to be closer to the WISE shapes, but the SDSS z -band images are generally of significantly lower signal-to-noise. Since we use the same galaxy profiles as used in the r -band “cModelMag” measurements, our measurements can be used consistently with those mags. When the “fracDev” deVaucoulers-to-total fraction is zero or one, our measurements are also consistent with the SDSS “modelMag” measurements for all bands.

It is a pleasure to thank Adam Myers, John Moustakas and Abhishek Prakash for early testing and feedback.

DWH was partially supported by the NSF (grant IIS-1124794), NASA (grant NNX12AI50G) and the Moore–Sloan Data Science Environment at NYU.

This publication makes use of data products from the Wide-field Infrared Survey Explorer, which is a joint project of the University of California, Los Angeles, and the Jet Propulsion Laboratory/California Institute of Technology, and NEOWISE, which is a project of the Jet Propulsion Laboratory/California Institute of Technology. WISE and NEOWISE are funded by the National Aeronautics and Space Administration.

This publication makes use of data from the Sloan Digital Sky Survey III. Funding for SDSS-III has been provided by the Alfred P. Sloan Foundation, the Participating Institutions, the National Science Foundation, and the U.S. Department of Energy Office of Science. The SDSS-III web site is <http://www.sdss3.org/>.

SDSS-III is managed by the Astrophysical Research Consortium for the Participating Institutions of the SDSS-III Collaboration including the University of Arizona, the Brazilian Participation Group, Brookhaven National Laboratory, Carnegie Mellon University, University of Florida, the French Participation Group, the German Participation Group, Harvard University, the Instituto de Astrofísica de Canarias, the Michigan State/Notre Dame/JINA Participation Group, Johns Hopkins University, Lawrence Berkeley National Laboratory, Max Planck Institute for Astrophysics, Max Planck Institute for Extraterrestrial Physics, New Mexico State University, New York University, Ohio State University, Pennsylvania State University, University of Portsmouth, Princeton University, the Spanish Participa-

tion Group, University of Tokyo, University of Utah, Vanderbilt University, University of Virginia, University of Washington, and Yale University.

This research used resources of the National Energy Research Scientific Computing Center (NERSC), which is supported by the Office of Science of the U.S. Department of Energy under Contract No. DE-AC02-05CH11231.

This research has made use of NASA’s Astrophysics Data System.

A. Description of our catalog contents

Our output files are row-by-row parallel to the SDSS *photoObj* files, and are named *photoWiseForced*. For example, the SDSS *photoObj* file containing objects observed in run 1000, camera column 1, field 100, in data reduction version 301, is found in the file⁵ `photoObj/301/1000/1/photoObj-001000-1-0100.fits` and our results are found in the file `301/1000/1/photoWiseForced-001000-1-0100.fits` where both of these files contains 368 rows, describing row-by-row the same objects.

The *photoWiseForced* files include the following columns:

`has_wise_phot` (boolean) True for SDSS sources that were photometered in WISE. The object must be PRIMARY in SDSS for this to be set. When this column is False, all other columns have value zero.

`ra, dec` (floats) J2000.0 coordinates from SDSS.

`objid` (string) Object identifier from SDSS.

`treated_as_pointsource` (boolean) The SDSS source is a galaxy (`objc_type == 3`) but was treated as a point source for the purposes of forced photometry. If you want an optical/WISE color, it would be best to use the SDSS PSF mags, not the model mags, for these objects.

`pointsource` (boolean) The SDSS source is a point source (`objc_type == 6`).

`coadd_id` (string) The unWISE coadd tile name, for example “3570p605”

`x, y` (float) Zero-indexed pixel coordinates of the source on the unWISE image tile (2048 × 2048 pixels).

⁵Or at the URL <http://data.sdss3.org/sas/dr10/boss/photoObj/301/1000/1/photoObj-001000-1-0100.fits>

w1_nanomaggies (float) WISE flux measurement for this object. Note that these are in the native WISE photometric system: Vega, not AB. A source with magnitude 22.5 in the Vega system would have a **w1_nanomaggies** flux of 1.⁶

w1_nanomaggies_ivar (float) WISE formal error as inverse-variance. Note that this formal error does not include error due to Poisson variations from the source. As such, it is most appropriate for faint objects.

w1_mag, **w1_mag_err** (floats) Vega magnitude and formal error in the forced photometry. These are simple conversions from the “nanomaggies” columns above.

w1_prochi2, **w1_pronpix** (floats) Profile-weighted chi-squared and number-of-pixels values. “Profile-weighted” means that these are weighted according to the profile of the source in the WISE images (eg, weighted by the point-spread function for point sources; weighted by the galaxy profile convolved by the point-spread function for galaxies). The column **w1_prochi2** is supposed to measure the quality of fit at the location of the source. Note that **w1_pronpix** effectively counts the fraction of the source that was inside the image, and should be close to unity for all sources.

w1_proflux (float) profile-weighted, the amount of flux contributed by other nearby sources. This will be zero for isolated sources, but can be larger than **w1_nanomaggies** if this source is blended with a brighter source.

w1_profracflux (float) equal to **w1_proflux** divided by **w1_nanomaggies**; the amount of flux at the location of this source that is due to other sources, relative to the flux of this source.

w1_npix (integer) The number of pixels included in the fit.

w1_pronexp (float) The number of WISE exposures included in the unWISE coadd at the location of this source. This is a proxy for the depth (which is also reflected in the formal error).

plus corresponding columns for **w2**, **w3**, and **w4**.

REFERENCES

Agarwal, S. *et al.*, 2012, Ceres Solver, <http://code.google.com/p/ceres-solver>

Ahn, C. P. *et al.*, 2013, ApJS, 211, 17; arXiv:1307.7735

⁶ The WISE team’s suggested conversions to AB are available here: http://wise2.ipac.caltech.edu/docs/release/allsky/expsup/sec4_4h.html#conv2ab

- Bovy, J. *et al.*, 2012, ApJ, 749, 41; arXiv:1105.3975
- Dawson, K.S. *et al.*, 2013, AJ, 145, 10; arXiv:1208.0022
- Eisenstein, D. J. *et al.*, AJ, 142, 72; arXiv:1101.1529
- Hogg, D.W. & Lang, D., PASP, 125, 719; arXiv:1210.6563
- Lang, D., 2014, AJ, 147, 108; arXiv:1405.0308
- Lawrence, A. *et al.*, 2007, MNRAS, 379, 1599; arXiv:astro-ph/0604426
- Lupton, R. H. *et al.*, ADASS X, 269; arXiv:astro-ph/0101420
- Mainzer, A. *et al.*, 2011, ApJ, 731, 53; arXiv:1102.1996
- Mainzer, A. *et al.*, 2014, ApJ, 792, 30; arXiv:1406.6025
- Martin, D. C. *et al.*, 2005, ApJ, 619, L1; arXiv:astro-ph/0411302
- Meisner, A. and Finkbeiner, D., ApJ, 781, 5; arXiv:1312.0947
- Wright, E. L. *et al.*, 2010, AJ, 140, 1868; arXiv:1008.0031
- Yan, L. *et al.*, 2013, AJ, 145, 55; arXiv:1209.2065
- York, D. G. *et al.*, 2000, AJ, 120, 1579; arXiv:astro-ph/0006396